



THE UNIVERSITY *of* EDINBURGH

Edinburgh Research Explorer

Inducible developmental reprogramming redefines commitment to sexual development in the malaria parasite *Plasmodium berghei*

Citation for published version:

Kent, R, Modrzynska, K, Cameron, R, Philip, N, Billker, O & Waters, A 2018, 'Inducible developmental reprogramming redefines commitment to sexual development in the malaria parasite *Plasmodium berghei*' Nature Microbiology. DOI: 10.1038/s41564-018-0223-6

Digital Object Identifier (DOI):

[10.1038/s41564-018-0223-6](https://doi.org/10.1038/s41564-018-0223-6)

Link:

[Link to publication record in Edinburgh Research Explorer](#)

Document Version:

Peer reviewed version

Published In:

Nature Microbiology

General rights

Copyright for the publications made accessible via the Edinburgh Research Explorer is retained by the author(s) and / or other copyright owners and it is a condition of accessing these publications that users recognise and abide by the legal requirements associated with these rights.

Take down policy

The University of Edinburgh has made every reasonable effort to ensure that Edinburgh Research Explorer content complies with UK legislation. If you believe that the public display of this file breaches copyright please contact openaccess@ed.ac.uk providing details, and we will remove access to the work immediately and investigate your claim.



1 **Inducible developmental reprogramming redefines commitment**
2 **to sexual development by a malaria parasite.**

3 *Robyn S Kent^{1,2}†, Katarzyna K Modrzynska^{1,3} †*, Rachael Cameron¹, Nisha Philip¹, Oliver Billker^{3*},*
4 *Andrew P. Waters^{1*}*

5
6 ¹: Institute of Infection, Immunity and Inflammation, University of Glasgow, Glasgow, G12 8TA, UK

7 ²: Department of Microbiology and molecular genetics, University of Vermont, Burlington, VT 05405, USA

8 ³: Wellcome Trust Sanger Institute, Hinxton, Cambridge, CB10 1SA, UK

9 † contributed equally

10 * co-corresponding

11
12 **Upon invading a mammalian red blood cell, a malaria parasite can replicate asexually or**
13 **transform into a gametocyte, responsible for disease transmission. Despite the key role of**
14 **gametocytes in the parasite life cycle, little is known about the mechanism regulating their**
15 **numbers and development. Here we show that inducible overexpression of a critical**
16 **transcription factor, AP2-G, is sufficient to convert asexual parasites efficiently into fertile**
17 **gametocytes. This discovery allowed us to redefine the time frame of commitment and the**
18 **sequence of transcriptional changes including the observation that gender partitioned**
19 **transcription is evident within 6 h of induction of gametocyte development. These data**
20 **provide entry points for further detailed characterization of processes critical to malaria**
21 **transmission.**

22 The ability to produce multiple, specialised cell types based on one genotype is typically
23 associated with multicellular organisms but can be found in all branches of the tree of life. The
24 causative agent of malaria, an apicomplexan parasite from the *Plasmodium* genus, is
25 characterised by a complex life cycle involving a number of morphologically different stages
26 adapted to different niches in its mammalian host or anopheline mosquito vector. These stages

27 undergo linear transitions with one notable exception: intracellular blood stages, which are
28 associated with all symptoms of malaria, enter one of two developmental pathways. Upon entry
29 into a red blood cell (RBC), parasites either replicate asexually forming a schizont (which contains
30 multiple merozoites able to invade new RBCs leading to an increase in parasitaemia), or develop
31 into sexual forms, male or female gametocytes, responsible for transmission to the mosquito
32 vector. The extent of gametocytogenesis varies in response to multiple environmental factors¹,
33 implying a significant flexibility in fate determination at the level of the individual cell. The
34 molecular mechanisms and stimuli regulating this process, however, remain poorly understood,
35 the recent advance demonstrating the role of the human serum component,
36 lysophosphatidylcholine in repression of gametocytogenesis notwithstanding².

37 In multiple model systems, differentiation into a particular cell type is triggered by key
38 transcription factors acting as switches between different developmental pathways^{3,4}. Previously
39 AP2-G, a transcription factor from the apicomplexa-specific apiAP2 family, was shown to be
40 necessary for gametocytogenesis in multiple *Plasmodium* species^{5,6}, and its absence resulted in
41 parasites unable to commit to sexual development (Fig. 1A). Here, we tested if overexpression of
42 this factor could increase gametocyte production and enable the investigation of the
43 uncharacterised, earliest stages of gametocyte development.

44 To create a tightly controlled conditional overexpression system, two different gene
45 expression modules were introduced into the genome of the rodent malaria parasite
46 *Plasmodium berghei*. First, a constitutively expressed split Cre recombinase (diCre) able to
47 catalyse recombination between *loxP* sequences when activated with rapamycin was introduced
48 into the *p230p* neutral locus of the parasite (Fig. 1B,C, S1)⁷. The resulting parasite line provided
49 efficient and rapid control over diCre activity, as shown by the ability to completely recombine a
50 test plasmid both *in vitro* and *in vivo*, switching the expression from green to red fluorescent
51 protein (Fig. 1D, E, S2). The second module included modified *loxP* sites (*lox66* and *lox71*)⁸ in a
52 head-to-head orientation flanking a strong constitutive promoter (*hsp70*) used to express a

53 selection marker (Fig. 1F). This module was inserted in front of the *ap2-g* ORF, interrupting and
54 uncoupling its native promoter (Fig. S3A). In this position the unidirectional induced lox
55 recombination event would invert the *hsp70* promoter and overexpress *ap2-g*.

56 Both modules were successfully inserted into a *P. berghei* reporter line containing a third
57 module that expressed green and red fluorescent reporter markers in male and female
58 gametocytes, respectively⁹, generating PB_{GAMi}⁻ PB_{GAMi} schizonts were synchronised *in vitro* and
59 grown *in vivo* with (PB_{GAMi}R+) or without (PB_{GAMi}R-) rapamycin. Both populations were analysed
60 at different time points using qPCR, light microscopy and flow cytometry (FACS). Recombination
61 was detected in the PB_{GAMi}R+ population immediately after induction and reached its maximum
62 at ~12 h, eliminating the unedited locus (Fig. 1G, S3B,C). In the PB_{GAMi}R- population, within 24 h
63 all parasites transformed into asexual schizonts, replicating the *ap2-g* ko phenotype and
64 resulting in an increase of parasitaemia (Fig. 2 A-D). In the PB_{GAMi}R+ population, in contrast,
65 PB_{GAMi}R+ parasites did not produce schizonts (Fig. 2A) or increase in [parasitaemia](#) (Fig. 2D).
66 Instead, many cells with gametocyte-like morphology appeared (Fig. 2A,B). Flow cytometry
67 confirmed expression of male and female reporter proteins in PB_{GAMi}R+ from 12 h post induction
68 (hpi; Fig. 2C and S4). The combined percentage of male and female gametocytes in the
69 population reached 70% in some experiments, and the total gametocyte proportion was always
70 significantly (P-value = 0.0021, [students unpaired t-test](#)) higher than in wt (Fig. 2B). Importantly,
71 GFP and RFP-positive cells emerged upon activation and formed male and female gametes,
72 respectively, confirming they are functional gametocytes (Fig. 2E). The relative ability of induced
73 male gametocytes to replicate their genomes upon activation was similar to wild type, although
74 their ability to go on to complete egress was reduced if compared to wild type (Fig. 2E). This
75 most likely reflects the fact that a reporter gene is necessarily an imperfect proxy for functional
76 maturity. In our system expression of the male marker from 12 h after induction (Fig. S4)
77 precedes functional maturity, and as a consequence, differences in the age distribution between

78 synchronous induced and asynchronous wildtype marker-positive male gametocytes must result
79 in differences in apparent functional maturity.

80 Experimental evidence from *P. falciparum* has suggested that commitment to
81 gametocytogenesis occurs in the blood stage cycle prior to the appearance of gametocytes
82 resulting in the production of a committed schizont/merozoite population destined to develop
83 into gametocytes following erythrocyte invasion¹⁰. To determine the period during which *P.*
84 *berghei* asexual parasites are sensitive to reprogramming, we induced *ap2-g* overexpression at
85 multiple time points during the 24 h cycle of asexual development (at 2, 4, 8, 12, 18, 22 h post
86 merozoite invasion). Parasites induced before 12 hpi could be transformed with decreasing
87 efficiency into gametocytes within the same developmental cycle (Fig. 2F, S5A). In marked
88 contrast, parasites induced after 12 hpi all developed into asexual schizonts and gametocyte
89 conversion was observed only following invasion, in the next cycle. The timing of induction did
90 not appear to have a marked effect on the cumulative number of gametocytes formed (Fig. S5A,
91 B). The male to female ratio in induced gametocytes was within the range observed in the
92 parental population (Fig. 2B), and any apparent shifts in sex ratio with time of induction (Fig. 2F)
93 may simply reflect the earlier upregulation of the male marker, as discussed above.

94 The inducible and synchronised sexual commitment provided an opportunity to assess
95 transcriptional changes in developing gametocytes. Synchronous schizonts (22hpi) were induced
96 *in vivo* with rapamycin to obtain a single wave of commitment after reinvasion and RNA-seq
97 libraries were prepared from PB_{GAMi}R⁻ and PB_{GAMi}R⁺ parasites harvested at 6h intervals between
98 0 and 30h post induction. Initially, data was used to examine the level of expression of functional
99 *ap2-g* transcript which was absent in PB_{GAMi}R⁻ population but detected in the PB_{GAMi}R⁺
100 population reaching its maximum at 12 h and exceeding native expression within the
101 population¹¹ within first 6 h (Fig. 3A, S6). Analysis of the remainder of the transcriptome
102 confirmed that at 30 hpi the PB_{GAMi}R⁻ population was similar to the transcriptome of asexual
103 schizonts, while PB_{GAMi}R⁺ was indistinguishable from purified gametocytes indicating that the

104 cells that did not develop into gametocytes either produced the gametocyte transcriptome or
105 were transcriptionally silent (Fig. 3B). The PB_{GAMI}R +/- populations diverged gradually starting
106 from 6 h (58 genes) to 30 h, when 2676 genes showed some level of differential regulation (Fig.
107 3C, Table S2). The dynamics of gene expression in PB_{GAMI}R+ parasites mirrored the expected
108 patterns of developing wild type gametocytes closely as indicated by gene ontology (GO) terms
109 associated with different time points (Fig. 3C, Table S3), which shifted from protein kinases and
110 motor proteins of the male gametocyte at 12 h, to cytoskeleton organisation (18 h) and the DNA
111 replication machinery (24 h). As expected, translationally repressed transcripts which are known
112 to be stored by the mature female gametocyte¹² were induced at later time points (Fig. S7).

113 Of particular interest was the group of 58 genes responding already at the 6 h time point. It
114 included conserved early gametocyte markers like *mdv1*¹³ as well as proteins potentially involved
115 in nucleic acid binding, including four zinc finger proteins, three RNA binding proteins, two
116 helicases and one other apiAP2 transcription factor (Fig. 3D). In comparison with the rest of the
117 genome this subset was significantly enriched (P= 1.387 e-05, Fisher exact tests) in genes
118 dispensable for asexual blood stages¹⁴ and many of its members are known to be specific to the
119 male or female sex in mature gametocytes¹⁵. The promoter regions of these genes were also
120 significantly (E = 1.1e-005) enriched in a GTGTAC(T/G) motif resembling closely the known DNA-
121 binding motif for the AP2 domain of AP2-G (Fig. 4E)¹⁶, suggesting at least some of them may be
122 direct downstream targets of AP2-G. Comparison with the available datasets from human
123 malaria *Plasmodium falciparum* revealed that almost all of these genes (35 out of the 49 with
124 identified syntenic orthologs) are upregulated in the early phase of gametocytogenesis (days 1 &
125 3) suggesting that the function of these genes is shared between different *Plasmodium* species
126 (Fig. 3D and S8). In contrast the genes that are up-regulated and co-expressed with *ap2-g* in *P.*
127 *falciparum*^{5,17} predominantly encode secreted proteins that are not present in the *P. berghei*
128 *genome* and thought to be associated with the extensive remodelling of the erythrocyte that is
129 uniquely undertaken by *P. falciparum* gametocytes¹⁸.

130 | To confirm a role of one of these [conserved, induced](#) genes in gametocytogenesis, we
131 | disrupted the predicted DEAD/DEAH helicase, PBANKA_0312700 (Fig. 4A, S9), which has a
132 | putative AP2-G binding site 650 bp upstream of its start codon and shows a robust
133 | transcriptional response at 6 hpi and a high level of expression in both male and female
134 | gametocytes. The mutant completely lacked mature male gametocytes as tested by FACS (Fig.
135 | 4B) and blood smears. Female gametocytes were, however, viable and able to transmit when
136 | crossed with a strain producing viable males (Fig. 4C). These findings were consistent with a
137 | predominant function for PBANKA_0312700 in male gametocyte development, although the
138 | reduction in ookinete conversion when compared to a fully viable female only strain (Fig. 4C)
139 | could also indicate a downstream role for this helicase in female gametocyte development or
140 | fertilisation.

141 | [In summary/Here](#), we have shown that inducible expression of AP2-G is sufficient to induce
142 | synchronous gametocytogenesis in a *Plasmodium* parasite, overriding the default asexual
143 | replication program and leading to the generation of functional gametocytes. Importantly, this
144 | conversion could be initiated within the same developmental cycle, proving that the fate of the
145 | young intraerythrocytic parasites is not irreversibly determined. This finding is seemingly at odds
146 | with previous reports from human parasites where the existence of sexually pre-committed
147 | schizonts producing next generation gametocytes has been reported^{19,17,10}. Our data may simply
148 | reflect significant differences in life cycle regulation between the two *Plasmodium* parasites -
149 | gametocytogenesis in *P. falciparum* uniquely takes ~12 days which is significantly longer than
150 | other *Plasmodium* spp. and *P. falciparum* gametocytes also possess a distinctive morphology.
151 | Alternatively our discovery suggests a more general plasticity in commitment and an extended
152 | time window during which environmental factors² and epigenetic pre-programming¹⁹ can impact
153 | the number of gametocytes. In that scenario a proportion of the schizonts would be predisposed
154 | to generate gametocytes but the final, irreversible commitment, would be a late event in asexual
155 | blood stage development in the next cycle depending solely on AP2-G acting as a switch

156 between the two transcriptional fates of the cell. According to that theory, also *P. falciparum*
157 parasites could be converted within the same cycle, but assays which would capture this
158 possibility have not been developed or tested. Instead our ability to bypass any upstream events
159 allowed us to reveal the early transcriptional programme downstream of AP2-G which appears
160 to be shared between the two parasites. Intriguingly, many of these early response genes have a
161 strongly sex specific expression profile¹⁵ or knock-out phenotype (including PBANKA_0312700
162 tested here), suggesting that AP2-G may regulate different subsets of genes in both male and
163 female precursors (Fig. 4D). This raises the possibility that commitment to the male or female sex
164 either precedes or is simultaneous with AP2-G mediated gametocytogenesis. This hypothesis has
165 also been proposed in recent work capturing early transcription events in *P. falciparum*²⁰ where
166 certain genes with sex-specific phenotypes were shown to be regulated independently of AP2-G.

167 In summary, the AP2-G overexpression system allows full control of *Plasmodium*
168 gametocytogenesis and generated new findings related to sexual commitment for future
169 investigation. Equally the application of the concept of the conditional inducible commitment
170 may be extended to other apicomplexan parasites in which sexual development is less tractable,
171 leading to basic new insights in these species.

172 **Materials and Methods:**

173 **Rodent malaria parasites and their maintenance.**

174 All experiments were performed using *Plasmodium berghei* 2.34 ANKA strain and its modifications
175 maintained in female, outbred mice (Theiler's Original (TO) or NIH-Swiss strain, Envigo) 8 -12 weeks of age.
176 The infections were initiated by intraperitoneal or intravenous injection of either the frozen parasite stock
177 or blood from an infected donor mouse and monitored daily using Giemsa stained thin blood smears. All
178 animal procedures were conducted under project licenses issued by the UK Home Office and with local
179 ethical approval.

180 **Generation of the mutant parasite lines.**

181 The non-fluorescent strain c115cy1 HP and its derivative 820, expressing GFP and RFP markers in male and
182 female gametocytes respectively⁹, were used to create diCre-expressing lines. The marker-free HP diCre
183 and 820 diCre lines were generated using the GIMO (gene-in marker out) approach described previously²¹
184 and presented in Fig. S1. Briefly, a positive-negative selection marker was inserted into the parasite's
185 neutral *p230p* locus via homologous recombination. After positive selection and cloning by serial dilution,
186 the second transfection followed by negative selection was used to replace the marker with the diCre
187 expression cassette, and a second cloning step was performed. The diCre-test line was generated by
188 transfecting HP diCre with a centromeric, single-copy plasmid containing a *hsp70* promoter, a floxed GFP
189 and RFP separated by a loxP site, as shown in Fig. 1G. The 820 diCre line was transfected with linear DNA
190 modifying the *ap2-g* locus as shown in Fig. S3 to generate PB_{GAMI}. A PBANKA_0312700 KO line was
191 generated in 820 parasites by replacing the gene with a positive-negative selection marker as shown in Fig.
192 S8.

193 All transfections were performed using an established *P. berghei* schizont electroporation protocol.
194 Parasites were grown to 1-6% parasitaemia in mice treated with 1.2 mg of phenylhydrazine (Sigma) two
195 days prior the infection, and collected by cardiac puncture before transfer to schizont media (RPMI 1640 +
196 L-glutamine + 25 mM HEPES, supplemented with 25% of foetal bovine serum, 10 mM sodium bicarbonate
197 and penicillin-streptomycin). After overnight culture at 37°C in an atmosphere of 5% CO₂, 5% O₂ and 90%
198 N₂, schizonts were isolated by 15 min of centrifugation at 500 g on a cushion of 55% Nycodenz (Lucron
199 Bioproducts). The schizonts were harvested from the interface were then electroporated with 1-10 µg of

200 linear DNA or plasmid using Amaxa Nucleofector device and Basic Parasite Nucleofector Kit 2 according to
201 manufacturer's instructions. Parasites were intravenously injected into new mice and recovered for 25 h
202 before selection with pyrimethamine (7 µg/ml in drinking water) or 5-fluorocytosine (1.5 mg/ml in the
203 drinking water, HP diCre and 820 diCre lines only). Selected parasites were recovered ~7 days post
204 transfection. All lines were cloned by limiting dilution before the next modification step.

205 **Genome editing in diCre parasites.**

206 *P. berghei* parasites were synchronised by overnight culture in schizont media and a Nycodenz gradient
207 was used to harvest schizonts, as described above. Purified schizonts were intravenously injected into
208 naive mice, where they maintained their synchronicity for 48 h. Rapamycin (Sigma) was dissolved in DMSO
209 to 4 mg/ml to generate the stock solution. DiCre test parasites were induced either *in vitro* and *in vivo*. For
210 *in vitro* induction, parasites were removed from the host by cardiac puncture 2 h post invasion (hpi) and
211 cultured in schizont media with 200 mM rapamycin. For *in vivo* induction the host animals were injected
212 intraperitoneally with 4 mg/kg of rapamycin 2 hpi. Parasites were harvested at various time points via tail
213 bleed or cardiac puncture for DNA and flow cytometry analysis. To generate a population of invading
214 merozoites overexpressing AP2-G, the PB_{GAMi} line was induced 22 hpi by 4 mg/kg of rapamycin injection
215 and its development was analysed in the next invasion cycle, unless specified otherwise. In each case, an
216 uninduced control population of parasites was analysed in parallel.

217 **DNA extraction for PCR or qPCR genotyping:**

218 To extract parasites from host blood, ~1 ml of heparinised whole blood was collected by cardiac puncture.
219 Leucocyte depletion was achieved by filtration through two sequential Plasmodipur filters (Europroxima)
220 according to the manufacturer's instructions. Remaining cells were resuspended in 10 volumes of pre-
221 chilled erythrocyte lysis buffer (150 mM NH₄Cl; 10 mM KHCO₃; 1 mM EDTA) and incubated on ice for 15
222 min. After lysis, parasites were pelleted by centrifugation for 8 min at 450 g and washed with 1x
223 phosphate buffered saline until complete removal of the coloration of supernatant and either stored at -
224 20°C for later DNA isolation or processed immediately.

225 In the second part of the protocol, the fresh or frozen parasite pellet was resuspended in 700 µl TNE buffer
226 (50 mM Tris-HCl, pH 7.4, 100 mM NaCl, 0.1 mM EDTA), supplemented with 200 µg RNAse and 1% SDS. This
227 mixture was incubated for 10 – 15 min at 37°C after which 200 µg proteinase K was added and the solution
228 incubated for a further 1 hour. Then a standard phenol and chloroform extraction protocol followed by

229 ethanol precipitation²² was used to extract the DNA from the lysate. Quality and concentration of the
230 nucleic acids were measured using a UV-Vis spectrophotometer (NanoDrop, Thermo Scientific).

231 **PCR genotyping.**

232 Genotyping strategies for genetically modified parasites are presented in Fig. S1, S2, S3 and S9 and the
233 primer sequences are given in the Table S1. All PCR reactions were performed using *Taq* DNA Polymerase
234 (NEB) and the following PCR program: 94°C 30 s//94°C 30 s/Tm°C 30 s/72°C 1min // x 30/72°C 10 s/4°C,
235 where Tm°C was a annealing temperature specific for each primer pair. PCR products were resolved on a
236 1% agarose gel supplemented with 1:10,000 SYBR Safe reagent and visualised using Gel Doc XR+ Gel
237 Documentation System.

238 **QPCR genotyping.**

239 QCR primers were designed as shown in Figures S2 and S3 and are shown in Table S1. The amplification
240 reaction was set up using 50 ng of DNA and QuantiTect Sybr Green PCR Kit (Qiagen) according to the
241 manufacturer's instructions. The reaction was incubated in StepOne Real-Time PCR System (Applied
242 Biosystems) using the following program: 95°C 10min s//95°C 15 s/60°C 1 min//x 40/95°C 15 s/60°C 1
243 min/gradient +0.3°C/95°C 15 s.

244 At least three technical replicates of each measurement were taken. A neutral sequence present in both
245 induced and uninduced sample was amplified as a reference and DNA from uninduced population was
246 used as control. The fold change calculations were based on the $\Delta\Delta Ct$ method
247 (docs.appliedbiosystems.com/pebiidocs/04371095.pdf).

248 **Western blot analysis of diCre production:**

249 Protein pellets (isolated as described for the DNA extraction) were suspended in 5x pellet volume of RIPA
250 lysis buffer (50 mM Tris-HCl, pH 8.0, 150 mM NaCl, 1 mM EDTA, 0.5 % sodium deoxycholate, 0.1 % SDS , 1
251 % triton X-100) and incubated on ice for ~30 min. The lysate was spun for 10 min at 4°C, at 14,000 rpm and
252 the supernatant was combined with 4x SDS gel-loading buffer (62.5 mM Tris-H₃PO₄, pH 7.5, 1 mM EDTA, 2
253 % SDS, 10 mM DTT, 1 mM NaN₃ and 33% glycerol) and fresh 15% β -mercaptoethanol. Samples were
254 boiled at 100°C for 5 min and loaded on SDS-PAGE gradient gel (Biorad). Electrophoresis was performed
255 using Mini-PROTEAN Tetra cell electrophoresis chamber (Qiagen) for 2 h at 120 V. The resolved proteins
256 were transferred on Whatman nitrocellulose membrane using a trans-blot electrophoretic transfer system
257 according to the manufacturer's protocol, blocked with 5% milk PBST and probed with the antibodies

258 against FKBP-12 (1:500), Cre (1:500) and enolase (1:1000) (all Abcam), followed by a compatible HRP-
259 labelled secondary antibody. Enhanced chemiluminescence system (ECL) was used to visualise the proteins
260 on X-ray film.

261 **Flow cytometry analysis diCre activity and gametocyte production:**

262 Red blood cells for analysis were collected from tail drops, cardiac puncture or parasite cultures. Cells
263 were suspended in pre-warmed rich PBS with Hoechst 33342 dye and stained for 30 min at 37°C. Stained
264 samples were washed and resuspended in flow cytometry buffer (10% rich PBS, 1 mM EDTA in PBS) and
265 analysed using LSR-II flow cytometer (Becton Dickinson) with following emission/excitation settings:
266 Hoechst (DAPI, yellow laser, 350 nm) 450/50, GFP (FITC 488 nm) 488/10 and RFP (PE 561 nm) 585/15. At
267 least 500,000 events were acquired for each sample. Initial gating was performed using forward and side
268 scatter to exclude the events below the size and granularity thresholds of red blood cells. Then FCS-H FCS-
269 W gating served to isolate single red blood cells and followed by Hoechst staining selecting parasite-
270 infected cells as shown in Fig. S4A. For the 820 line and its derivatives, GFP and RFP gates were used to
271 select the male and female gametocytes respectively. For the diCre-test line the GFP, RFP and
272 bifluorescent populations were selected to show different stages of excision as shown in Fig. S2D. In each
273 experiment involving 820 modifications uninfected blood and wt 820 line were used as controls. In
274 fluorescence switching experiments both non-fluorescent parasites and lines constitutively expressing GFP
275 or RFP only (with appropriate strength promoters) only were used as controls (Fig. S2E).

276 **Exflagellation/emergence**

277 Tail drops of blood were collected in 500 µl 37°C schizont media (as above, unactivated) or 21°C ookinete
278 media (RPMI1640, 10% FCS, xanthurenic acid, activated) and incubated at the appropriate temperature for
279 30 min. Ter119 PEcy7 ([https://www.thermofisher.com/antibody/product/TER-119-Antibody-clone-TER-
280 119-Monoclonal/25-5921-82](https://www.thermofisher.com/antibody/product/TER-119-Antibody-clone-TER-119-Monoclonal/25-5921-82)) and Hoechst were added to a final concentration of 1:200 and a total
281 volume of 700 µl and intensively vortexed. Samples were incubated at their appropriate temperature for
282 an additional 20 min, vortexing every 5 min. Stained samples were washed in 500 µl of rPBS and
283 resuspended in 500 µl of FACS buffer for analysis. Male and female gametocytes were identified by
284 their GFP and RFP signal respectively using the gating presented in Fig. S4A. Gametocytes were considered

285 unactivated if positive for PEcy7 Ter119 staining and activated if this staining is negative. Only gametocytes
286 were included in quantification of activation.

287 **Time course of variable gametocyte induction and flow cytometry quantification**

288 Mice were injected with synchronised PB_{GAMi} parasites and induced *in vivo* with rapamycin at multiple time
289 points post invasion (2, 6, 8, 12, 18, 22 h) as described previously. Samples were obtained from tail drops
290 where parasitaemia (Hoechst 33342-positive cells) and percentage of male (GFP) and female (RFP)
291 gametocytes were quantified every 4 h from 8 h post invasion using flow cytometry. Since sex specific
292 fluorescence makers became detectable only from 16 h post invasion (Fig. S4B), any gametocytes
293 originating from the second cycle after induction would become detectable only after 40 hpi post invasion
294 (24 h cycle + 16 h maturation;). Therefore we considered the highest measurement taken before 40 hpi as
295 the number of gametocytes produced within the first cycle. The last measurement taken 64 hpi was
296 considered as the total number of gametocytes produced within both cycles.

297 **Time course of gametocyte induction, RNA extraction and RNA-seq library preparation.**

298 Mice were injected with synchronised PB_{GAMi} parasites and induced with rapamycin at 22 h as described
299 previously. Parasites were harvested at different time points post induction via cardiac puncture, filtered,
300 extracted from RBC and washed in 1xPBS as for DNA isolation. Parasite pellets were resuspended in 1ml of
301 Trizol reagent (Ambion) lysed for 10 min at room temperature and stored at -80°C for later RNA extraction.
302 Complete RNA was isolated from the samples using Trizol/chloroform extraction followed by isopropanol
303 precipitation²² and its concentration and integrity was verified using Agilent Bioanalyzer (RNA 6000 Nano
304 kit) and NanoDrop 1000 spectrophotometer. 1-2 µg of total RNA from each sample (or complete sample if
305 the yield was lower) was used for mRNA isolation (Magnetic mRNA Isolation Kit, NEB). First strand cDNA
306 synthesis was performed using the SuperScript III First-Strand Synthesis System and a 1:1 mix of Oligo(dT)
307 and random primers (Invitrogen). The DNA-RNA hybrids were purified using Agencourt RNACleanXP beads
308 (Beckman Coulter) and the second cDNA strand was synthesized using a 10 mM dUTP nucleotide mix, DNA
309 Polymerase I (Invitrogen) and RNaseH (NEB) for 2.5 h at 16°C. The long cDNA fragments were purified and
310 fragmented using a Covaris S220 system (duty cycles = 20, intensity = 5, cycles/burst = 200, time = 30s).
311 The ~200 bp long fragments were end-repaired, dA-tailed and ligated to “PCR-free” adapters (Kozarewa et
312 al., 2009) with index tags using NEBNext Modules according to the manufacturer’s instructions. Excess
313 adapters were removed by two rounds of clean-up with 1 volume of Agencourt AMPure XP beads. Final

314 libraries were eluted in 30 µl water, quality-controlled using Agilent Bioanalyzer (High Sensitivity DNA chip)
315 digested with USER enzyme (NEB) and quantified by qPCR. For some libraries additional 5 cycles of PCR
316 amplification were performed, using KAPA HiFi HotStart PCR mix and Illumina tag-specific primers to
317 obtain enough material for sequencing. Pools of indexed libraries were sequenced using an Illumina
318 HiSeq2500 system (100 bp paired-end reads) according to manufacturer's manual. All samples were
319 generated in duplicates or triplicates and uninduced controls were always generated and processed in
320 parallel. Raw data is available through GEO database repository (study GSE110201).

321 **RNAseq data analysis:**

322 The generation of raw data in the form of *.cram files quality control and adapter trimming was
323 performed using the default analysis pipelines of the Sanger Institute. The raw data was transformed into
324 paired *.fastq files using Samtools software (ver. 1.3.1). The generated reads were re-aligned to
325 *Plasmodium berghei* genome (PlasmoDB-30 release) in a splice aware manner with HISAT2²³ using --
326 known-splicesite-infile option within the splicing sites file generated based on the current genome
327 annotation. Resulting *.bam files were sorted and indexed using Samtools and inspected visually using
328 Integrated Genome Viewer (ver. 2.3.91). HT-seq python library²⁴ was used to generate reads counts for all
329 genes for further processing. Differential expression calculation and correlation analysis was performed
330 and visualised using R studio software (v. 1.0.136) with DESeq2, ggplot2 and GMD packages²⁵.
331 The reference schizont and gametocytes transcriptome datasets were downloaded from²⁶ and compared
332 to the generated samples using Spearman's rank correlation coefficient. The enrichment for the
333 translationally repressed genes in different differentially expressed datasets was performed using Fisher
334 exact test. For the analysis of male and female specificity and growth rates the data from¹⁵ and¹⁴
335 respectively was used. Growth rate above 0.8 was considered normal, between 0.8 and 0.2 – decreased
336 and below 0.2 the gene was considered essential. Gene was considered male/female specific if its
337 expression in the gametocytes of given sex was at least 10 fold greater than in the opposite and sex as well
338 as in the asexual parasites. DOZI translationally repressed genes were defined as the ones enriched in both
339 DOZI and CITH RIP-~~seq~~ **ChIP** datasets²⁷. Comparison with *P.falciparum* data was performed using the
340 available PF datasets^{6,28} and synteny information¹¹. Genes were considered as overexpressed in early
341 gametocytes stages in their expression was at least 2-fold greater than in matched asexual population²⁸.

342

343 *De novo* regulatory motif discovery was performed using DREME software²⁹ and sequences 2 kb upstream
344 of the translation sites of the genes upregulated 6 h post rapamycin induction as the input set and the
345 | promoters of the remaining genes in the genome as the reference set.
346

347 **References:**

- 348 1. Meibalan, E. & Marti, M. Biology of Malaria Transmission. *Cold Spring Harb. Perspect. Med.* **7**,
349 a025452 (2017).
- 350 2. Brancucci, N. M. B. *et al.* Lysophosphatidylcholine Regulates Sexual Stage Differentiation in the
351 Human Malaria Parasite *Plasmodium falciparum*. *Cell* **171**, 1532–1544.e15 (2017).
- 352 3. Soufi, A. *et al.* Pioneer Transcription Factors Target Partial DNA Motifs on Nucleosomes to Initiate
353 Reprogramming. *Cell* **161**, 555–568 (2015).
- 354 4. Thomson, M. *et al.* Pluripotency Factors in Embryonic Stem Cells Regulate Differentiation into
355 Germ Layers. *Cell* **145**, 875–889 (2011).
- 356 5. Sinha, A. *et al.* A cascade of DNA-binding proteins for sexual commitment and development in
357 *Plasmodium*. *Nature* **507**, 253–7 (2014).
- 358 6. Kafsack, B. F. C. *et al.* A transcriptional switch underlies commitment to sexual development in
359 malaria parasites. *Nature* **507**, 248–52 (2014).
- 360 7. Jullien, N., Sampieri, F., Enjalbert, A. & Herman, J.-P. Regulation of Cre recombinase by ligand-
361 induced complementation of inactive fragments. *Nucleic Acids Res.* **31**, e131 (2003).
- 362 8. Albert, H., Dale, E. C., Lee, E. & Ow, D. W. Site-specific integration of DNA into wild-type and
363 mutant lox sites placed in the plant genome. *Plant J.* **7**, 649–59 (1995).
- 364 9. Mair, G. R. *et al.* Universal features of post-transcriptional gene regulation are critical for
365 *Plasmodium* zygote development. *PLoS Pathog.* **6**, e1000767 (2010).
- 366 10. Bruce, M. C., Alano, P., Duthie, S. & Carter, R. Commitment of the malaria parasite *Plasmodium*
367 *falciparum* to sexual and asexual development. *Parasitology* **100 Pt 2**, 191–200 (1990).
- 368 11. Otto, T. D. *et al.* A comprehensive evaluation of rodent malaria parasite genomes and gene
369 expression. *BMC Biol.* **12**, 86 (2014).
- 370 12. Mair, G. R. *et al.* Regulation of sexual development of *Plasmodium* by translational repression.
371 *Science* **313**, 667–9 (2006).
- 372 13. Lal, K. *et al.* *Plasmodium* male development gene-1 (mdv-1) is important for female sexual
373 development and identifies a polarised plasma membrane during zygote development. *Int. J.*
374 *Parasitol.* **39**, 755–61 (2009).

- 375 14. Bushell, E. *et al.* Functional Profiling of a Plasmodium Genome Reveals an Abundance of Essential
376 Genes. *Cell* **170**, 260–272.e8 (2017).
- 377 15. Yeoh, L. M., Goodman, C. D., Mollard, V., McFadden, G. I. & Ralph, S. A. Comparative
378 transcriptomics of female and male gametocytes in Plasmodium berghei and the evolution of sex
379 in alveolates. *BMC Genomics* **18**, 734 (2017).
- 380 16. Campbell, T. L., De Silva, E. K., Olszewski, K. L., Elemento, O. & Llinás, M. Identification and
381 genome-wide prediction of DNA binding specificities for the ApiAP2 family of regulators from the
382 malaria parasite. *PLoS Pathog.* **6**, e1001165 (2010).
- 383 17. Poran, A. *et al.* Single-cell RNA sequencing reveals a signature of sexual commitment in malaria
384 parasites. *Nature* **551**, 95–99 (2017).
- 385 18. Tibúrcio, M., Sauerwein, R., Lavazec, C. & Alano, P. Erythrocyte remodeling by Plasmodium
386 falciparum gametocytes in the human host interplay. *Trends Parasitol.* **31**, 270–278 (2015).
- 387 19. Brancucci, N. M. B. *et al.* Heterochromatin Protein 1 Secures Survival and Transmission of Malaria
388 Parasites. *Cell Host Microbe* **16**, 165–176 (2014).
- 389 20. Painter, H. J., Carrasquilla, M. & Llinás, M. Capturing in vivo RNA transcriptional dynamics from the
390 malaria parasite *Plasmodium falciparum*. *Genome Res.* **27**, 1074–1086 (2017).
- 391 21. Lin, J. *et al.* A Novel ‘Gene Insertion/Marker Out’ (GIMO) Method for Transgene Expression and
392 Gene Complementation in Rodent Malaria Parasites. *PLoS One* **6**, e29289 (2011).
- 393 22. Chomczynski, P. A reagent for the single-step simultaneous isolation of RNA, DNA and proteins
394 from cell and tissue samples. *Biotechniques* **15**, 532–4, 536–7 (1993).
- 395 23. Kim, D., Langmead, B. & Salzberg, S. L. HISAT: a fast spliced aligner with low memory requirements.
396 *Nat. Methods* **12**, 357–360 (2015).
- 397 24. Anders, S., Pyl, P. T. & Huber, W. HTSeq - A Python framework to work with high-throughput
398 sequencing data. *Bioinformatics* **31**, 166–9 (2014).
- 399 25. Love, M. I., Huber, W. & Anders, S. Moderated estimation of fold change and dispersion for RNA-
400 seq data with DESeq2. *Genome Biol.* **15**, 550 (2014).
- 401 26. Modrzynska, K. *et al.* A Knockout Screen of ApiAP2 Genes Reveals Networks of Interacting
402 Transcriptional Regulators Controlling the Plasmodium Life Cycle. *Cell Host Microbe* **21**, 11–22
403 (2017).

- 404 27. Guerreiro, A. *et al.* Genome-wide RIP-Chip analysis of translational repressor-bound mRNAs in the
405 Plasmodium gametocyte. *Genome Biol.* **15**, 493 (2014).
- 406 28. Young, J. a *et al.* The Plasmodium falciparum sexual development transcriptome: a microarray
407 analysis using ontology-based pattern identification. *Mol. Biochem. Parasitol.* **143**, 67–79 (2005).
- 408 29. Bailey, T. L. DREME: motif discovery in transcription factor CHIP-seq data. *Bioinformatics* **27**, 1653–
409 9 (2011).

410

411 **Acknowledgments:**

412 We thank R. Menard and Daniel Bargieri for the diCre-test plasmid utilised in this study and to Mandy
413 Sanders and WTSI sequencing service for assistance with RNA-seq samples processing. KKM is supported
414 by Wellcome Trust and the Royal Society (Ref 202600/Z/16/Z). RSK is supported by BBSRC (Ref
415 BB/J013854/1). APW is supported by the Wellcome Trust (Refs: 083811_ & 107046). OB is supported by
416 Wellcome Trust Sanger Institute (Ref WT098051).

417

418 **Competing financial interests:**

419 Authors declare no competing financial interests.

420

421 **Author's contributions:**

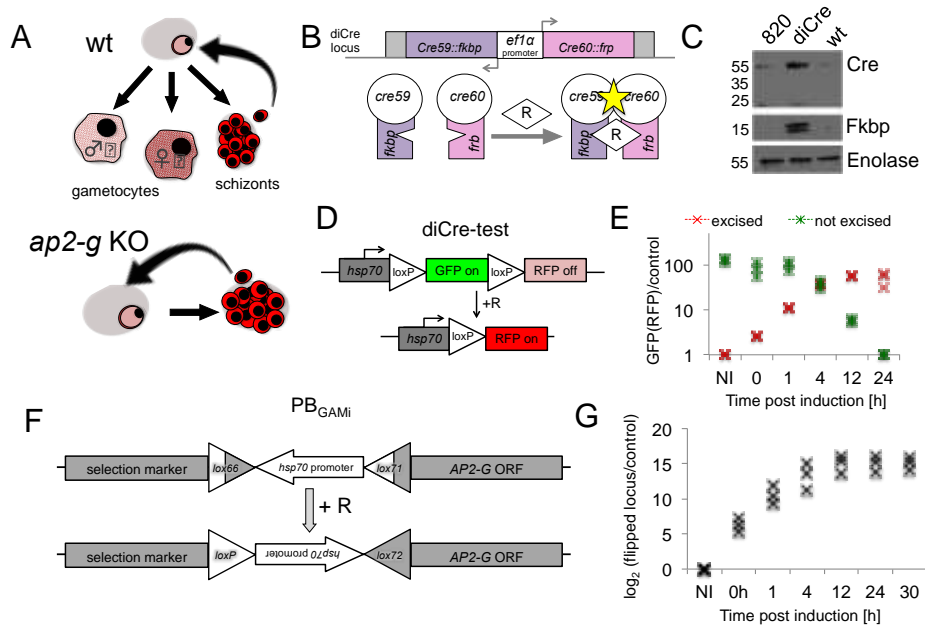
422 RSK generated and phenotyped HP diCre, diCre test and PBANKA_0312700 lines, performed
423 phenotyping experiments on PB_{GAMi} line and generated parasites for transcriptome sequencing.

424 KKM generated the AP2-G overexpression construct and PB_{GAMi} line, performed phenotyping
425 experiments on PB_{GAMi} line, generated RNA-seq libraries and performed RNA-seq data analysis.

426 RC generated 820 diCre and GIMO lines and parasites for transcriptome sequencing. NP
427 performed the ookinete conversion assay for PBANKA_0312700 line. OB and APW led and
428 supervised the study. KKM and APW wrote the manuscript with contributions from other
429 authors.

430

431

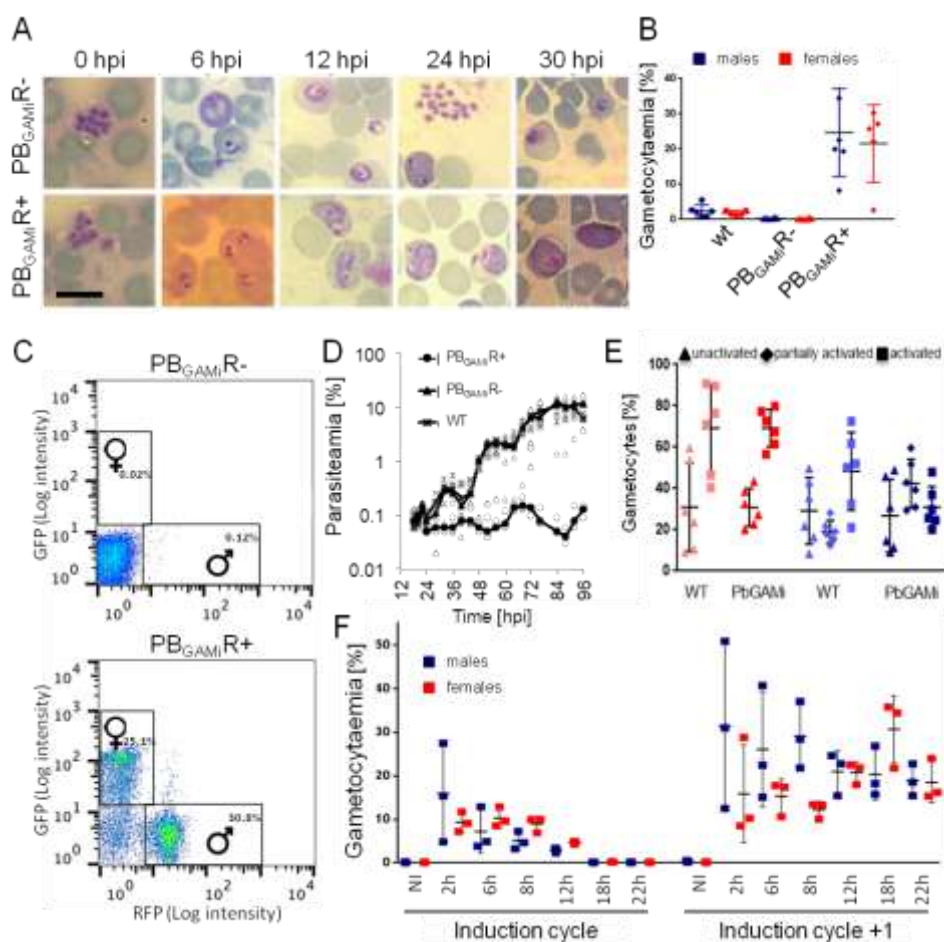


432

433 **Fig. 1: Establishment of AP2-G overexpression system:**

- 434 A. Top: cartoon depicting the three developmental fates of a newly invaded ring stage parasite, from left: male
 435 gametocyte, female gametocyte and schizont (comprised of daughter merozoites, capable of invading new red
 436 blood cells and forming new rings). Bottom: Parasites missing *ap2-g* undertake only asexual development.
- 437 B. Top: the cassette inserted in the *P. berghei* 820 line expressing two Cre fragments fused to FKBP and FRB
 438 respectively driven by the bidirectional *ef1a* promoter. Bottom: Principle of reconstitution of Cre recombinase
 439 activity upon addition of Rapamycin (R).
- 440 C. Western analysis showing expression of the two DiCre system fragments in the cloned PB_{GAMi} line. Cre antibody
 441 shows Cre60::FRB and FKBP antibody shows Cre59::FKBP. [Three independant blots were completed with similar](#)
 442 [results.](#)
- 443 D. Design of construct to test DiCre activity.
- 444 E. QPCR quantification of edited and unedited test plasmid sequences in diCre-test parasites at different time points
 445 after rapamycin induction. Three technical replicates of the samples generated within the same time course are
 446 shown. [At each time point DNA was harvested from an independently infected animal.](#)
- 447 F. Cartoon of *ap2-g* locus in PB_{GAMi} parasites before (top) and after (bottom) editing event.

448 G. qPCR quantification of the edited *ap2-g* locus in the PB_{GAMI} parasites. Three technical replicates of the samples
449 generated within the same time course are shown. [At each time point DNA was harvested from an independently](#)
450 [infected animal.](#)



451

452 **Fig. 2: AP2-G overexpression results in gametocyte conversion:**

453 A. Parasite morphology in Giemsa-stained thin blood smears in $PB_{GAMI}R^-$ (top) and $PB_{GAMI}R^+$ (bottom) population

454 demonstrating evident production of gametocytes in the induced parasites. Representative pictures from [53](#)
 455 [independent biological replicates for each time point experiments](#) are shown. **** I don't know where the scale bar**
 456 [came from as my images didn't have one!! **](#)

457 B. Gametocyte conversion rates in $PB_{GAMI}R^-$ and $PB_{GAMI}R^+$ parasites compared to the parental line. Gametocytaemia

458 shown as percentage of infected cells expressing male (blue)/female (red) markers in FACS analysis 30 h post

459 induction. Means, standard deviations and individual data points from [55](#) independent biological replicates are

460 [shown](#).

461 C. FACS profiles of $PB_{GAMI}R^-$ and $PB_{GAMI}R^+$ parasites 30h after induction, representative for [5](#) [biologically](#) independent

462 experiments. Male and female parasite populations gating is shown.

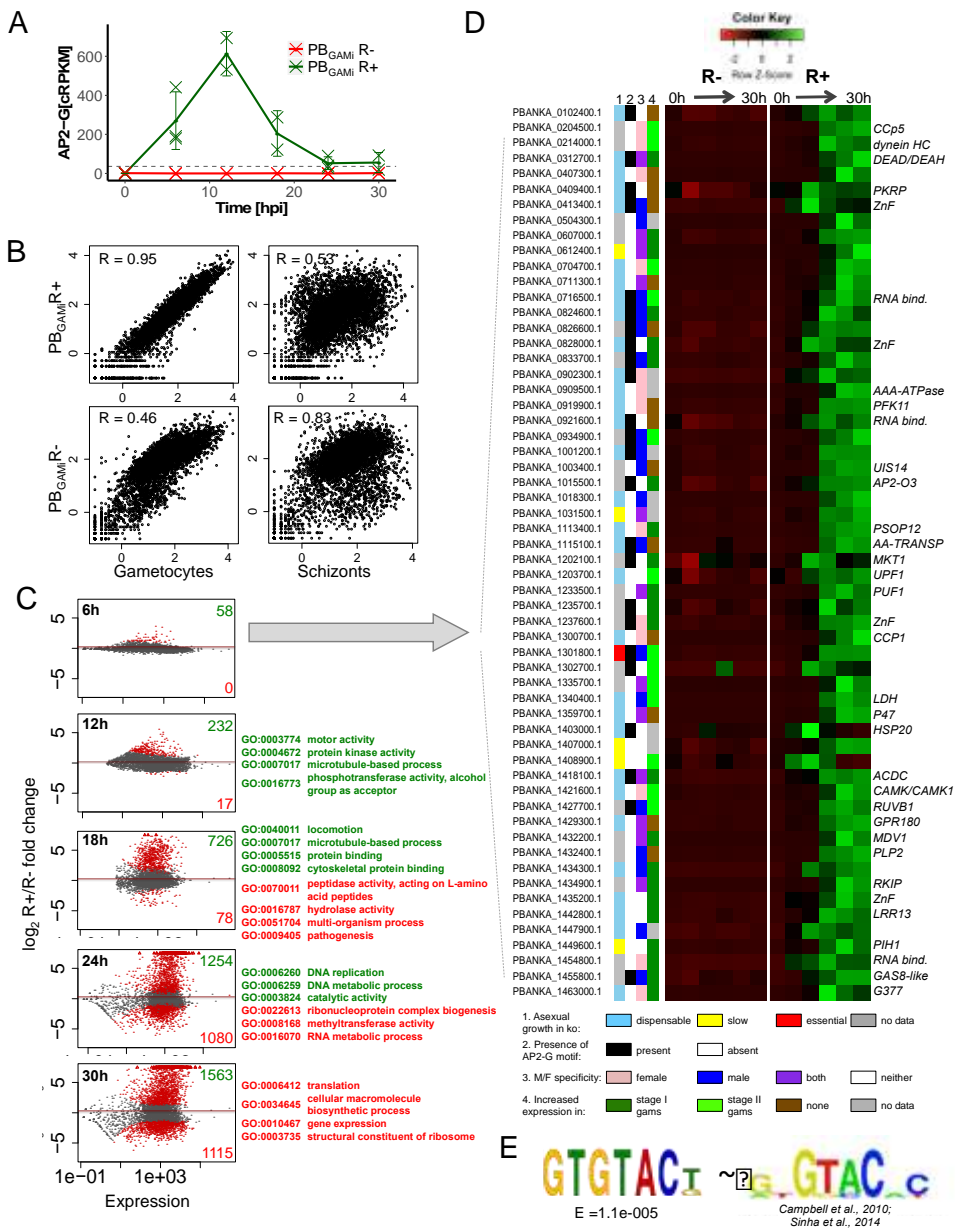
Comment [RK1]: I removed one replicate (randomly) from the one that had 6 so they are all the same.

463 D. Parasitaemia in PB_{GAMI}R-/R+ population compared to wt parasites defined as percentage of DNA positive red blood
464 cells in FACS analysis. Median and individual measurements from 3 independent biological replicates are shown.

465 E. Percentage of unactivated ~~(U)~~, activated ~~(A)~~ and partially activated ~~(P)~~ cells in wild-type (WT) and PB_{GAMI}R+
466 gametocytes. Full activation is defined as successful production of male gametes and their emergence out of the
467 blood cells (exflagellation). Partial activation of male gametocytes is identified when DNA replication has occurred
468 (increase in Hoechst 33342 intensity) but exflagellation from the red blood cell has not occurred. Means, standard
469 deviations and individual data points from five independent biological replicates are shown. Statistical significance
470 assessed using unpaired two-tailed t-test.

471 F. Gametocyte conversion rates in PB_{GAMI} parasites induced *in vivo* at the different time points post-invasion. Total
472 proportion of gametocytes generated within the same cycle (maximum measurement until 40hpi) and after
473 subsequent reinvasion (64 hpi) is shown for the same infection. NI =non-induced.

474



475

476 **Fig. 3: Transcriptome changes in PB_{GAMI}-R- and PB_{GAMI}-R+ parasites reveal gametocyte-specific transcriptional**
477 **program**

478 A. Expression of *ap2-g* transcript in PB_{GAMI}-R- and PB_{GAMI}-R+ populations. Corrected rpkM calculated as seen in Fig. S6.

479 Means, standard deviations and individual data points from >2 independent biological replicates are shown.

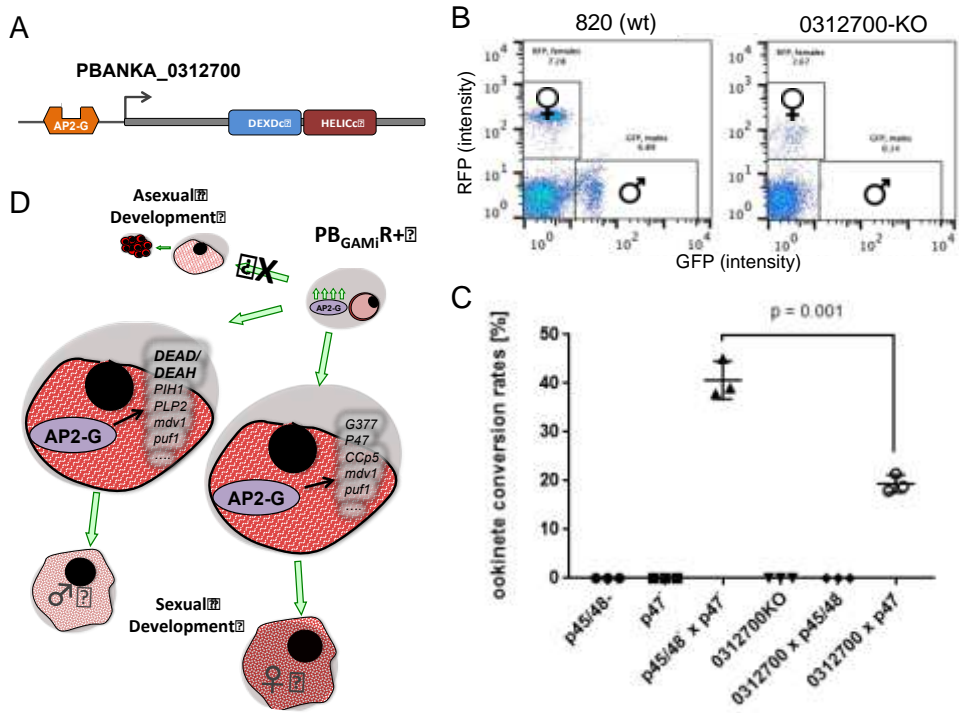
480 Horizontal, black dashed line indicates maximal native *ap2-g* RNA expression in WT population¹¹.

481 B. Comparison of transcriptomes (rpkm's) from PB_{GAMI}R- and PB_{GAMI}R+ populations 30 hpi to purified gametocytes and
482 schizonts transcriptomes. R = Spearman's rank correlation coefficient.

483 C. Differential expression analysis between PB_{GAMI}R- and PB_{GAMI}R+ populations at different time points. Plots show log₂
484 fold change of gene expression vs. expression levels, with differentially expressed genes marked in red. Numbers
485 of genes overexpressed in PB_{GAMI}R- (red) and PB_{GAMI}R+ (green) and example GO terms enriched within each group
486 next to each graph. All samples for transcriptome analysis were generated from three independent time-course
487 experiments.

488 D. Genes responding early to AP2-G overexpression. Shown are: knock-out growth phenotype in asexual blood
489 stages¹⁴, sex specificity of expression in *P. berghei*¹⁵, gametocyte specificity in *P. falciparum*²⁸, presence of AP2-G
490 motif(s) in 2 kb upstream of the start codon, and gene expression profile through the time course. Available gene
491 symbols are shown on the right of the expression profile.

492 E. The DNA motif enriched upstream of genes in panel D (left) compared with the known AP2-G binding motif^{5,16}
493 (right)



494

495

Fig. 4: PBANKA_0312700 is an AP2-G-induced gene involved in gametocyte development:

496

A. PBANKA_0312700 gene structure with conserved helicase domains and putative AP2-G binding motif marked.

497

B. Representative FACS analysis showing loss of male gametocytes in the PBANKA_0312700 KO. Experiment was replicated >3 times.

499

C. Ookinete conversion in PBANKA_0312700 KO crossed with line producing only viable females (*p48/45*) or males

500

(*p47*), showing that the defect gametocyte development is male specific. Means, standard deviations and

501

individual data points from three independent biological replicates are shown.

502

D. Model of AP2-G function in gametocyte commitment.

503